Semi-empirical Prediction of the Flow Structure Behind a Longitudinally Oscillating Cylinder Based on Surface Vorticity Analysis

S. J. XU[1], M. H. WANG[2], Y. ZHOU[3*,] & J. Y. TU[4]
[1]School of Aerospace, Tsinghua University, Beijing, China, 100084
[2] State Key Laboratory for Turbulence and Complex System, Peking University, Beijing, China, 100871
[3]Department of Mechanical Engineering, The Hong Kong Polytechnic University, Hung Hom, Kowloon, Hong Kong
[4]School of Aerospace, Mechanical and Manufacturing Engineering, RMIT University, Australia

Abstract

The 2-D incompressible N-S equations in a moving cylindrical coordinate were reduced to a linear boundary vorticity equation on the cylinder surface with the no-slip condition applied. The solution to the reduced vorticity equation unveils that vorticity generated by the cylinder surface comprises of two components: i) unsteady and anti-symmetrical component, dependent of the cylinder oscillation; ii) steady alternating component associated with the natural vortex shedding. The competition of the two components, interactions among cylinder-vortices and vortex-vortex result in the occurrence of the flow modes. In the first-stage work, a semi-empirical prediction of the occurrence of the S-II mode is in agreement with previously reported experimental and numerical data. Further analysis is under way to predict the occurrence of all other flow modes.

1. Introduction

When a flow passes an oscillating cylinder, vorticity is generated by the cylinder surface because of viscous effect. The oscillating cylinder transfers the kinetic energy and vorticity to the flow. Vortices may shed from the cylinder and move downstream. The oscillating cylinder may reattach the vortices to change the convection velocity and shape of the vortices. These vortices also interact with each other to form a stable vortex street. Investigations involving a longitudinally oscillating cylinder in a cross-flow have been rather limited. Five typical flow structures, referred to as S-I, S-II, A-I, A-III and A-IV mode behind a longitudinally oscillating cylinder, had been reported in the previous experiments [1-4] or numerical simulations [5, 6], respectively. These studies have uncovered many important aspects of physics associated with a longitudinally oscillating cylinder wake, but the full-understanding of the issue is much less satisfied. Questions can be asked, e.g., when will each flow mode occur? Why do the flow modes render so

inerratic flow patterns such as symmetrical binary vortices in the S-II mode? To answer these questions, we are in attempt to study the vorticity generated by the cylinder surface, which unveils the vortex formation; and then to analyze interactions of vortices-cylinder, vortex-vortex in this paper. It is expected to predict the occurrence of flow structures behind an oscillating cylinder in longitudinal direction.

2. Review of flow structures behind a longitudinal oscillating cylinder

Figure 1 presents the flow visualization pictures about the five flow structures [3]. For a small combination of A/d and f_e/f_s, one unstable symmetric vortex street is formed behind the cylinder. The flow structure was referred to the S-I mode (Fig. 1a), which is breaking up quickly. The A-I mode visualized in Fig. 1b will occur with increased the combination of A/d and f_e/f_s. Vortices are now shed anti-symmetrically from the cylinder, forming a staggered vortex street. At a higher the combination of A/d and f_e/f_s, the flow structure is characterized by one row of binary vortices and one row of single vortices. Each binary vortex consists of one pair of counter-rotating vortices. The flow mode is referred as the A-III mode (Fig. 1c). The A-IV mode occurs at a little bit higher combination of A/d and f_e/f_s compared with the A-III mode. One staggered binary vortex street is formed. The difference between the A-III and the A-IV mode is that vortices in both rows are binary ones, each consisting of a pair of counter-rotating vortices (Fig. 1d). As the combination of A/d and f_e/f_s is increased over a critical value, the S-II mode occurs. This flow structure is also symmetrical to the centerline of the wake but apparently different from the S-I mode flow structure; it is composed of binary vortices. Each binary vortex encloses two counter-rotating vortices. Xu et al. [4] referred to the flow structure as the S-II mode (Fig. 1e).

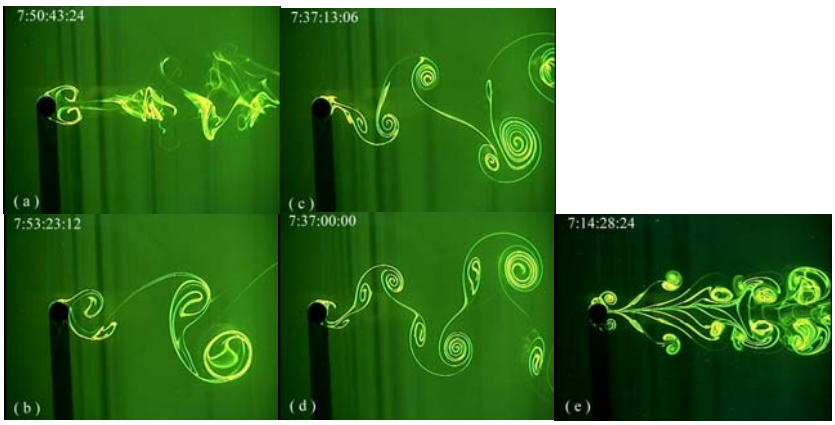

FIGURE1-The flow visualization photographs of five typical flow structures behind a longitudinally oscillating cylinder: (a) S-I; (b) A-I; (c) A-III; (d) A-IV and (e) S-II (Xu 2003).

3. Vorticity dynamics on the cylinder surface

Consider a moving cylindrical co-ordinate system, which is fixed on the oscillating cylinder (Figure 2). The cylinder displacement in the streamwise direction may be written as $X(t) = A\cos(2\pi f_e t + \varphi_0)$, where φ_0 is the initial phase angle of the oscillating cylinder.

Let us consider a flow of low Reynolds number, which is approximately two-dimensional around the cylinder. Thus, the 2-D incompressible N-S equations can be given by

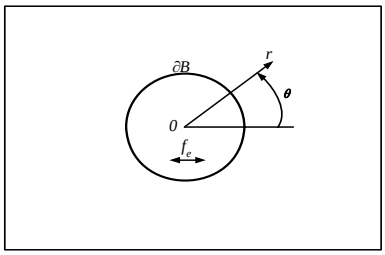

FIGURE-2 Moving reference frame fixed on the cylinder.

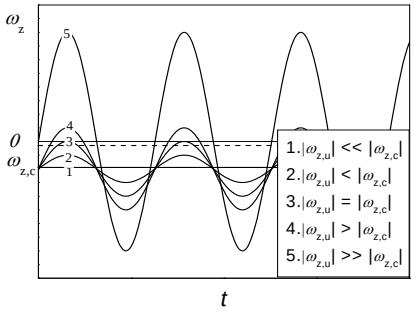

FIGURE-3 Five combinations of $\omega_{z,u}$ and $\omega_{z,c}$.

$$\frac{\partial \mathbf{V}}{\partial t} + \mathbf{V} \cdot \nabla \mathbf{V} = -\frac{1}{\rho}\nabla p + \nu \nabla^2 \mathbf{V} - \boldsymbol{a}\,, \tag{1a}$$

and $$\nabla \cdot \mathbf{V} = 0\,, \tag{1b}$$

where $\mathbf{V}$ is the flow velocity vector, p is pressure, ρ is the fluid density，t is time and $\boldsymbol{a}$ is the acceleration vector of the cylinder, $a_x = \ddot{X}(t) = -4\pi^2 f_e^2 A\cos(2\pi f_e t + \varphi_0)$. The vorticity equation is given by

$$\frac{\partial \omega}{\partial t} + (\mathbf{V} \cdot \nabla)\omega - (\omega \cdot \nabla)\mathbf{V} = \nu \nabla^2 \omega - \nabla \times \boldsymbol{a} \tag{2}$$

In the cylindrical co-ordinate system, eliminating the terms related to pressure p in (1) with considering no-slip condition and then substitute to (2), one may obtain the vortcity generated on the surface after quite exhaustive algebra. For the surface of $r = d/2$, the vorticity can be obtained as

$$\omega_z = \frac{4\pi f_e A}{d}\sin\left(2\pi f_e t + \varphi_0\right)\sin\theta + \omega_{z,c}(\theta) = \omega_{z,u}(t,\theta) + \omega_{z,c}(\theta) \tag{3}$$

It is evident from Eq (3) that the voticity generated by the cylinder surface comprises of two components: i) an unsteady component, $\omega_{z,u}(t,\theta)$, which is anti-symmetrical, or symmetrical in terms of magnitude, about the flow centreline, and ii) a steady component, $\omega_{z,c}$, which is the solution for the case of a stationary cylinder subjected to a steady uniform cross flow ($\omega_{z,u}(t,\theta) \equiv 0$). Here, $\omega_{z,u}(t,\theta)$ is dependent on the cylinder oscillation and $\omega_{z,u}(t,\theta) \equiv 0$ in case of a stationary cylinder. In other words, the voriticy created by the surface of an oscillating cylinder in a uniform flow may be investigated as two steps, i.e., study of a cylinder oscillating in a fluid at rest and study of the stationary cylinder in a steady uniform cross flow, respectively. From the flow stability point of view, the two stabilities or the two components of ω_z compete and interact, which determines where, when and how the flow separates from the cylinder to

roll up into vortex. There are five combinations of $\omega_{z,u}(t,\theta)$ and $\omega_{z,c}$ are possible and are illustrated in Fig. 3, viz.

1) In case of $|\omega_{z,u}| << |\omega_{z,c}|$, the cylinder oscillation is negligible, then $\omega_z \approx \omega_{z,c}$, that is, ω_z is approximately independent of time, given by the horizontal line in Fig. 3 (line 1). The flow structure is the same as that behind a stationary cylinder. In this situation, lock-on could not occur because $|\omega_{z,c}|$ domains the vorticity. At a low Reynolds number, $|\omega_{z,c}|$ might be very small, lock-on could occur if $\omega_{z,u}$ domains the vorticity creation. Thus, ω_z tends to be symmetric about the *x*-axis (see the dashed line in Fig.3), which determines the separated flow is approximately symmetrical. However, this separated symmetrical flow mode is unstable and collapses rapidly since the competition between $\omega_{z,u}$ and $\omega_{z,c}$ is even, as the observed S-I mode (Fig 1a).

2) If the cylinder is forced to oscillate, with $|\omega_{z,u}| < |\omega_{z,c}|$ and $\omega_{z,u}$ appreciable compared with $\omega_{z,c}$ (see line 2 in Fig. 3), $\omega_{z,c}$ is predominant and ω_z assumes the sense of $\omega_{z,c}$. Accordingly, the flow separation should display to a certain degree the feature of the Karman vortex street, showing the A-I mode structure (Fig. 1b). With increasing cylinder oscillation (e.g. increasing f_e/f_s at a fixed A/d), $\omega_{z,u}$ (symmetrical) may compete more vigorously with $\omega_{z,c}$ (alternating), resulting in a different flow separations, e.g., the A-III or A-IV mode (Fig. 1). Indeed, the alternate nature of the vortices is discernible for A-I and A-III or A-IV modes. However, the A-III or A-IV mode embraces the vortical structure of twin vortices. To further analyze the occurrence of the flow modes, one is resorted to understand how the separated vortices interact with the oscillating cylinder.

3) For $|\omega_{z,u}|$ is very close to $|\omega_{z,c}|$, $|\omega_{z,u}| \approx |\omega_{z,c}|$ (line 3 in Fig. 3), a new equilibrium state, namely the A-IV mode, may occur, and ω_z attains the sense of $\omega_{z,c}$. In this situation, the vortices are rearranged into one staggered binary vortex street. In the first half of one cycle, the upper shear layer around the cylinder separates to form a vortex, which crosses the centreline to join the vortex shed earlier from the lower side of the cylinder, forming one binary vortex in the lower row. A similar process occurs in the other half of one cycle [3].

4) As $|\omega_{z,u}|$ exceeds $|\omega_{z,c}|$ considerably (line 4), the vortices symmetrically separates from the cylinder. The structure of symmetrically arranged vortices dominates and the stability of the vortex street should be controlled by $\omega_{z,u}$. It implies that the S-II mode occurs.

5) In the limiting case, $|\omega_{z,u}| >> |\omega_{z,c}|$ (line 5), the flow around the cylinder is only controlled by the cylinder oscillation and the steady streaming [7, 8] around the cylinder occurs, where the high frequency oscillation of a cylinder in a fluid initially at rest causes a secondary flow through the action of viscosity in the boundary layer.

The symmetry of the flow structure in Cases 4) and 5) may be also inferred from the boundary vorticity flux, which represents the vorticity diffuses away from the cylinder surface per unit time and unit area [9]:

$$\sigma = \nu \frac{\partial \omega_z}{\partial \theta} = 2\pi^2 f_e^2 Ad \cos(2\pi f_e t + \varphi_0)\cos\theta - \frac{d}{2\rho}\frac{\partial p}{\partial r}. \quad (4)$$

Equation (4) can be easily obtained from Eq. (1) along with the no-slip condition (3). In a situation where the oscillation is very large, that is, $f_e A$ is large enough, σ is symmetrical about the *x*-axis.

It worth noting that (3) is valid on the surface of the cylinder. Out of the surface, the non-linear parts in (2) won't be zero. In this situation, the interaction between the two components of (3) is non-linear.

4 Prediction of the S-II mode

The S-II mode is displaying a remarkable symmetric binary vortex street. This symmetry implies a negligible mean and fluctuating lift on the cylinder and is potentially of engineering significance. Therefore, it would be interesting to examine the onset condition of this flow structure. For $U_\infty \neq 0$, the onset of the binary vortex can only occur as $|\omega_{z,u}|$ exceeds $|\omega_{z,c}|$ considerably (line 3 in Fig 4). Furthermore, the maximum magnitude, $\omega_{z,u\max}$, of $\omega_{z,u}$ should reach a certain level, which occurs at $\theta = \pm 90^o$, i.e., the top and bottom points of the cylinder, based on Eq. (3). As discussed in [4], the two vortices of one binary vortex are generated when the cylinder moves oppositely to and along U_∞, respectively. The formation of the binary vortex must be associated with a sufficiently large cylinder velocity (or sufficiently large $\omega_{z,u\max} = 4\dot{X}_{\max}/d$) relative to U_∞ even when the cylinder moves in the same direction as U_∞. Figure 5 shows schematically the flow velocity distributions, at the top of the cylinder, due to the cylinder oscillation in fluid at rest and a uniform flow over the stationary cylinder, respectively, and the combined velocity $u(y)$. Since $\frac{\partial v}{\partial x} << \frac{\partial u}{\partial y}$, the vorticity generated is given by

$$\omega_z = \frac{\partial v}{\partial x} - \frac{\partial u}{\partial y} \approx \frac{\partial u}{\partial y}. \quad (5)$$

Hence, $\int_0^\delta \omega_z dy \approx \int_0^\delta \frac{\partial u}{\partial y} dy = u(\delta) - u(0) = u(\delta)$, where δ is the boundary layer thickness. Then, the onset of the binary vortex may be stated as

$$u(\delta) = 2\pi f_e A - U_\infty > u_c, \quad (6)$$

where $u_c > 0$ is the critical velocity at which the vorticity generated in the boundary layer reaches an adequate strength to form a vortex and separates from the cylinder. Relation (6) may be rewritten in terms of a relative Reynolds number, viz.

$$\Delta \mathrm{Re} = \frac{(2\pi f_e A - U_\infty)d}{\nu} > \frac{u_c d}{\nu} = \mathrm{Re}_c, \tag{7}$$

where Re_c is the critical Reynolds number.

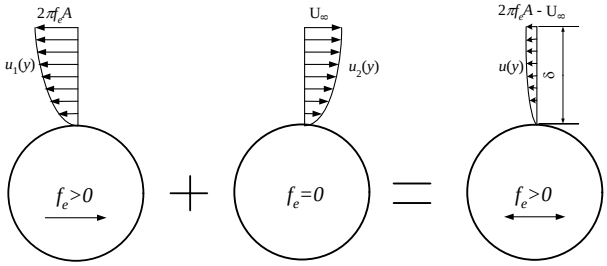

FIGURE-4 Velocity distributions at the top of the oscillating cylinder

In case of a stationary cylinder, $\Delta Re = -\frac{U_\infty d}{\nu}$ is negative and no binary vortex will form since the condition (7) cannot be met.

In order to estimate the onset conditions of the binary vortex, Re_c in (7) has to be determined. It is well known that for a stationary cylinder the creeping flow regime (no flow separation) occurs for $Re < 5$. For $5 < Re < 40$, the shear layers around the cylinder separate steadily and merge downstream, forming symmetric and steady twin vortices or a closed near-wake [10]. For $Re > 40$, unsteady vortex shedding starts. Once the cylinder is forced to oscillate, the flow is unsteady and the critical Reynolds number for the shear layers to separate from the cylinder in a steady flow should be invalid. This number should be smaller than 5 in view of the enhanced flow instability. Nevertheless, we will see later that the reduced Re_c has very limited influence on the occurrence of the binary vortex street. For convenience, assume $Re_c = 5$. Condition (7) may be reformulated as

$$f_e / f_s \geq \frac{(1 + \frac{\mathrm{Re}_c}{\mathrm{Re}})}{2\pi St(\mathrm{Re})}\left(\frac{A}{d}\right)^{-1} = (f_e / f_s)_c, \tag{8}$$

where St is the Strouhal number in a stationary cylinder case, depending on Re, i.e., $St = St(Re)$, $(f_e/f_s)_c$ is the threshold value for the occurrence of the S-II mode flow structure. The relationship $St = St(Re)$ is well documented in the literature [11, 12]. Based on (8), $(f_e/f_s)_c$ is inversely proportional to A/d, in qualitative agreement with the observation from the experimental data that, as A/d increases, the S-II mode starts to occur at a smaller f_e/f_s. In the limiting case, if $A/d \to \infty$ (e.g. towing a cylinder through a water tank at some acceleration in the same direction as mean flow), $f_e/f_s \to 0$; if $A/d = 0$ (a stationary cylinder), $f_e/f_s \to \infty$, that is, it is impossible to generate the binary vortex. If (8) is not satisfied, i.e. $\Delta \mathrm{Re} = \frac{(2\pi f_e A - U_\infty)d}{\nu} < \mathrm{Re}_c$, in case of a small $(2\pi f_e A - U_\infty)$, the modes other than the S-II mode flow structure then occur.

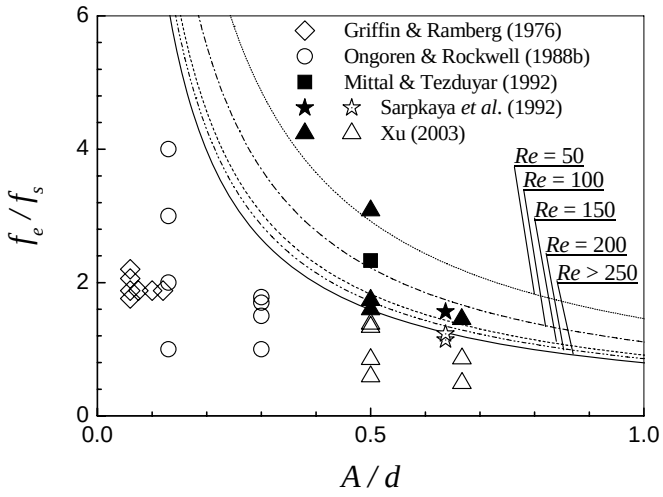

FIGURE-6 Prediction of the S-II mode flow structure. Solid symbols indicate S-II mode and open symbols represent other modes

For $40 < Re < 200$, $St\,(Re) = 0.21(1 - 21/Re)$ [12], (8) may be written as

$$f_e / f_s \geq \frac{(\mathrm{Re} + \mathrm{Re}_c)}{0.42\pi(\mathrm{Re} - 21)}\left(\frac{A}{d}\right)^{-1} = \left(f_e / f_s\right)_c \qquad 40 < \mathrm{Re} < 200\,. \tag{9a}$$

At a large *Re*, say > 250, $St\,(Re) \approx 0.2$, even we take $\mathrm{Re}_c \approx 5$, $\mathrm{Re}_c/\mathrm{Re} = 5/\mathrm{Re} \approx 0$, the *Re* effect on the occurrence of the S-II mode should be negligible. Eq. (8) can be then simplified, viz.

$$f_e / f_s \geq \left(f_e / f_s\right)_c \approx \frac{5}{2\pi}\left(\frac{A}{d}\right)^{-1}. \tag{9b}$$

Therefore, (8) or (9) is the condition for the occurrence of the S-II mode.

Figure 6 presents the prediction chart based on (9) together with available experimental data and numerical data obtained from Mittal & Tezdugar [5] at Re = 100 and Sarpkaya *et al.* [6] at Re = 800. The S-II mode flow structure occurs in the region above the curve. The open symbols represent the flow structures of the S-I, A-I, A-III and A-IV modes, while the solid symbol indicates the occurrence of the S-II mode. A number of comments can be made based on the chart. (1) As *Re* increases at an increment of 50, the curve translates downwards, indicating a dependence of the occurrence of the S-II mode on *Re*, but the translating increment becomes smaller for higher *Re*, suggesting a diminishing *Re* effect, in particular for *Re* > 250. (2) The predicted occurrence of the S-II mode is in good agreement with both experimental and numerical data. For $A/d = 0.5$ and $Re = 100$, the S-II mode is predicted from Eq. (8) to occur at $f_e/f_s = 1.05/[\pi\, St(Re)] \approx 0.334/St(100)$, where $St(100)$ represents the Strouhal number at $Re = 100$. This value was $0.35/St(100)$ based on Mittal & Tezdugar's numerical simulation [5]. Good agreement is

also evident between the prediction and Sarpkaya *et al.'* numerical data [6]. For $A/d = 0.5$ and $Re = 150$, the S-II mode is predicted from Eq. (8) to occur at $f_e/f_s \approx 1.7$, while observed experimentally at $f_e/f_s \approx 1.74$. Noting a small Re effect on this changeover for $Re \geq 150$, the agreement between previous numerical or present experimental data and the prediction of the occurrence of the S-II mode structure suggests that the choice of the critical Reynolds number ($Re_c = 5$) for the inception of the binary vortex formation is reasonable. (3) The occurrence of the S-II mode requires $f_e/f_s > 6.0$ for $A/d = 0.13$, $f_e/f_s > 2.7$ at $A/d = 0.3$, or $f_e/f_s > 0.83$ at $A/d = 0.96$, which may explain why Ongoren and Rockwell [2] and Cetiner & Rockwell[13] failed to observe this flow structure (Ongoren and Rockwell's f_e/f_s was up to 4 at $A/d = 0.13$ and did not exceed 1.8 at $A/d = 0.3$. Cetiner & Rockwell's f_e/f_s was 0.3 at $A/d = 0.96$). (4) Other than Re, initial conditions such as turbulence level, roughness of cylinder, etc. may affect the value of Re_c and hence the occurrence of the S-II mode.

5. Summary and further work

In this paper, the flow structures behind a longitudinally oscillating cylinder were analyzed based on the boundary vorticity theory. The analysis unveiled that vorticity generated by the cylinder surface comprises of two components: i) unsteady and anti-symmetrical component, dependent of the cylinder oscillation; ii) steady alternating component associated with the natural vortex shedding. The competition between the two components, interactions between cylinder and vortices, and interaction between vortex and vortex finally results in the five stable flow modes reported by the previous experimental studies. The prediction of the occurrence of the flow modes was conducted based on the solution. In the first-stage work, the prediction of the occurrence of the S-II mode is in good agreement with previously reported experimental and numerical data. Further analysis is under way to predict the occurrence of all other flow modes.

References

[1] GRIFFIN, O. M. and RAMBERG, S. E. 1976 *J. Fluid Mech.* **75**, 257-271.
[2] ONGOREN, A. and ROCKWELL, D. 1988a&b *J. Fluid Mech.* **191**, a:197-223, b: 225-245.
[3] XU S.J. 2003 "*Fluid-structure interactions of an oscillating cylinder in cross flow in the presence of a neighbouring cylinder*", Ph.D. thesis of the Hong Kong Polytechnic University.
[4] XU S.J., ZHOU Y and WANG M. H. 2006 *J. Fluid Mech.* (**in press**).
[5] MITTAL, S. & TEZDUYAR, T.E. 1992 *International Journal for Numerical methods in fluids*, **15**, 1073-1118.
[6] SARPKAYA, T., PUTZIG, C., GORDON, D., WANG, X. & DALTON, C. 1992 *Journal of offshore Mechanics and Artic Engineering*, **114**, 219-298.
[7] RILEY, N. 1975 *Journal of Fluid Mechanics*, **68**(4), 801-812.
[8] RILEY, N. 2001 *Annual Reviews of Fluid Mechanics*, **33**, 43-65.
[9] LIGHTHILL M.J. 1963 "Introduction: Boundary Layer Theory, in *Laminar Boundary Layer*", edited by L. ROSENHEAD, Oxford University Press, Oxford, UK, pp. 46-113.
[10] Zdravkovich, M. M. 1997 "*Flow around circular cylinders Vol. 1: Fundamentals*". Oxford University Press, England, pp 6-13.
[11] Blevins, D. 1994 "*Flow-induced vibration*". Krieger publishing company, Florida, USA. pp48.
[12] Chen, S. S. 1987 "*Flow-induced Vibration of Circular Cylinder Structures*". Hemisphere Publishing Corporation. pp.260.
[13]CETINER, O. & ROCKWELL, D. 2001. *J. Fluid Mech.* **427**, 1-59.